Domestication of a housekeeping transglycosylase for assembly of a Type VI secretion system

Yoann G Santin, E. Cascales

Domestication of a housekeeping transglycosylase for assembly of a Type VI secretion system[¶]

Yoann G. Santin and Eric Cascales*

Running title: Peptidoglycan remodeling for T6SS assembly

Keywords: secretion system, protein transport, multiprotein assembly, protein complex, peptidoglycan

Laboratoire d'Ingénierie des Systèmes Macromoléculaires (LISM), UMR 7255, Institut de Microbiologie de la Méditerranée, Aix-Marseille Univ – CNRS, 31 Chemin Joseph Aiguier, 13402 Marseille Cedex 20, France.

* e-mail: cascales@imm.cnrs.fr

[¶] This work is dedicated to Odette Santin.

Abstract

The Type VI secretion system (T6SS) is an anti-bacterial weapon comprising a contractile tail anchored to the cell envelope by a membrane complex. The TssJ, TssL and TssM proteins assemble a 1.7-MDa channel complex that spans the cell envelope, including the peptidoglycan layer. The electron microscopy structure of the TssJLM complex revealed that it has a diameter of ~ 18 nm in the periplasm, which is larger that the size of peptidoglycan pores (~ 2 nm), hence questioning how the T6SS membrane complex crosses the peptidoglycan layer. Here, we report that the MltE housekeeping lytic transglycosylase (LTG) is required for T6SS assembly in enteroaggregative *E. coli*. Protein-protein interactions studies further demonstrated that MltE is recruited to the periplasmic domain of TssM. In addition, we show that TssM significantly stimulates MltE activity *in vitro* and that MltE is required for the late stages of T6SS membrane complex assembly. Collectively, our data provide the first example of domestication and

activation of a LTG encoded within the core genome for the assembly of a secretion system.

Introduction

The cell envelope of Gram negative bacteria is crossed by multiprotein complexes that participate to the assembly of surface appendages (*e.g.*, the flagellum) or serve as channels for the passage of large molecules such as pili, DNA or protein effectors (*e.g.*, piliation, conjugation or secretion systems) [1]. These complexes are usually large and are anchored to both the inner and outer membranes [1]. However, the peptidoglycan layer represents a physical barrier for the assembly of these structures, as they are usually larger than peptidoglycan pores, estimated to have a diameter of ~ 2 nm [2]. Most of these systems have therefore evolved enzymes, called lytic transglycosylases (LTGs), that locally rearrange the cell wall [3-5]. LTGs cleave the glycan strands but have no action on peptide cross-links, therefore creating lateral separation of the peptidoglycan [6,7]. Endogeneous LTGs are involved in peptidoglycan synthesis, turnover, recycling and daughter cell separation [7-9]. By contrast, the LTGs dedicated to specific cell-envelope spanning complexes are called specialized LTGs [3-5,8]. The activity of these enzymes needs to be tightly controlled to avoid peptidoglycan breaches and cell lysis [8,10]. In addition, the LTG activity should be spatially controlled to create sufficient space at the site of assembly. The spatial activation of specialized LTGs is secured by their recruitment to the site of assembly through interactions with one or several components of the apparatus. The recruitment of specialized LTGs to their cognate apparatus has been exemplified in the case of several cell-spanning machineries: the *Rhodobacter sphaeroides* SltF LTG is recruited to the flagellar FlgJ subunit [11,12], the PleA protein localizes at the cell pole in *Caulobacter crescentus* and is required for the assembly of the polar pilus and polar flagellum [13], the VirB1-like LTG is recruited to the VirB8-like protein in Type IV secretion systems [4,14-19], and the EtgA LTG associates with the Type III secretion system EscI rod component [4,20-22]. Interestingly, in a few cases, machine subunits comprise an additional domain with LTG activity, such as the flagellar rod FlgJ protein [23-27] or the *Bordetella pertussis* T4SS PtlE subunit [28]. For several of these enzymes, it has been recently demonstrated that the transglycosylase activity is weak *in vitro* but stimulated in presence of its partner suggesting that binding to the cell-envelope spaning

structure specifically activates the enzymatic activity and hence controls localized peptidoglycan hydrolysis. The activity of the T3SS EtgA LTG is enhanced by co-incubation with the EscI rod subunit [22]. In the case of the *R. sphaeroides* flagellum, the activity of SltF is modulated by both FlgB and FlgF [29].

Recently, we determined the structure of the 1.7-MDa Type VI secretion system (T6SS) membrane complex from enteroaggregative *E. coli* (EAEC) using negative stain electron microscopy [30]. This complex spans the cell envelope, and its diameter was estimated to ~ 18 nm in the periplasm, suggesting that its proper insertion requires localized peptidoglycan rearrangement or degradation. However, no gene encoding LTG is encoded within T6SS gene clusters [31,32]. The T6SS is a sophisticated multiprotein machine that is widely distributed in Gram-negative bacteria and responsible for the delivery of toxin effectors in both prokaryotic and eukaryotic cells, hence participating in bacterial competition and pathogenesis [33-42]. It is constituted of a cytoplasmic tail complex that is evolutionarily, structurally and functionally related to contractile machines such as phages or pyocins [43-45]. The tail comprises an inner tube composed of Hcp hexamers stack on each other and wrapped into the contractile sheath formed by the polymerization of TssBC complexes [46-50]. The inner tube is tipped by the VgrG/PAAR complex that is used as a puncturing device to penetrate the target cell [47,51]. Once assembled, the sheath contracts and propels the Hcp/VgrG/PAAR needle complex, allowing effector delivery and target cell lysis [49,52-54]. The tail is built onto an assembly platform, the baseplate, constituted of the TssEFGK-VgrG subunits [55-57]. The baseplate docks to the membrane complex that both orientates the tail towards the cell exterior and serves as channel for the passage of the Hcp/VgrG/PAAR needle [30,56,58,59]. The membrane complex is composed of the TssJ, TssL and TssM proteins, each present in ten copies [30,60]. TssL and TssM are both inner membrane proteins, with soluble domains in the cytoplasm and periplasm respectively [58,61,62]. TssJ is an outer membrane lipoprotein [63] that interacts with the C-terminal domain of the TssM periplasmic region [64]. The assembly of the membrane complex starts with the initial positioning of the TssJ lipoprotein and progresses inward with the ordered addition of TssM and TssL [30]. Once assembled, the membrane complex recruits the TssA protein and the baseplate complex prior to tail/sheath polymerization [56,65]. In addition to span the cell envelope, the membrane complex is anchored to the cell wall by an additional component TagL, or an additional domain fused to the C-terminus of TssL, that shares homology to peptidoglycan-

binding proteins [60,66]. It is proposed that anchorage to the cell wall allows stabilization of the membrane complex, notably during sheath contraction. The negative stain electron microscopy structure of the EAEC TssJLM complex demonstrated that it is composed of a base comprising the cytoplasmic domains of TssL and TssM and forms a trans-envelope channel with ten arches and ten pilars constituted by the periplasmic domain of TssM and the TssJ lipoprotein [30]. The diameter of this complex in the periplasm is however incompatible with the size of peptidoglycan pores and we hypothesized that proper insertion or assembly of the T6SS membrane complex requires the action of a LTG. Recently, a study identified TagX, a T6SS-encoded peptidoglycan endopeptidase required for T6SS function in *Acinetobacter* species [67]. However, the *tagX* gene is not conserved and the vast majority of T6SS gene clusters does not encode peptidoglycan hydrolases. This observation raised the question on how these Type VI secretion systems deal with the peptidoglycan layer. Here, we show that the EAEC T6SS has domesticated the housekeeping MltE LTG for its assembly.

Results

Proper fonction of the EAEC T6SS requires the MltE housekeeping lytic transglycosylase.

To test whether peptidoglycan remodeling is required for assembly of the T6SS, cells were treated with Bulgecin A, a specific inhibitor of transglycosylases [68,69], and the release of Hcp in the culture supernatant, a marker of EAEC T6SS assembly and function [63], was probed by western-blot analyses. To avoid Hcp release by pre-assembled and active T6SS, we monitored the experiments in a strain deleted of the *tssM* gene but bearing a plasmid-borne wild-type *tssM* allele under the control of an inducible Tet promoter. In this strain, the basal expression of *tssM* is undetectable by western-blot and is not sufficient to support assembly of the T6SS. In presence of inducer, the T6SS is assembled and hence Hcp was detected in the culture supernatant (Fig. 1A). The addition of Bulgecin A in the medium prior to *tssM* induction did not impact TssM production but prevented Hcp release (Fig. 1A). This result demonstrates that the T6SS does not function when the activity of LTGs are inhibited, and suggests that the action of at least one endogeneous LTG is required for the assembly of this

apparatus. Using time-lapse fluorescence microscopy, we previously showed that the TssJLM membrane complex is used for several rounds of tail assembly and contraction [30]. To confirm this result, wild-type EAEC cells were washed to discard secreted Hcp proteins, and resuspended in medium supplemented with Bulgecin A, to prevent assembly of new T6SS membrane complexes. After 45 min of growth, the presence of Hcp in the supernatant was probed by western-blot analyses. We observed that Hcp was released, demonstrating that pre-assembled T6SS membrane complexes are not sensitive to treatment with Bulgecin A (Fig. 1B).

The EAEC 17-2 chromosome encodes 8 proteins with signature of LTGs. These include the soluble Slt70 and the membrane-bound MltA-E housekeeping lytic transglycosylases, as well as two putative LTGs: EtgA encoded within the T3SS gene island and the product of the EC042_2762 gene. To test the contribution of these proteins for the assembly of the EAEC T6SS, we generated knock-out strains in each of these genes, and tested the ability of these strains to support Hcp secretion. Western-blot analyses of cell-free culture supernatants showed that Hcp release was abolished in the *mltE* strain, suggesting that the outer-membrane anchored MltE lipoprotein (EC042_1244; gene accession number, GI: 284920999) is necessary for T6SS function in EAEC and that no redundancy occurs between the EAEC LTGs for the assembly of the T6SS (Fig. 2 and Fig. 3A).

The EAEC Sci-1 T6SS has recently been shown to provide a competitive advantage against other *E. coli* species [70]. Fig. 3B shows that the number of GFP^+ kanamycin-resistant *E. coli* K-12 prey cells recovered after co-culture with EAEC *mltE* cells is 4-log higher compared to co-culture with EAEC wild-type cells. This effect is comparable to that observed for a Δ*tssM* mutant. The $T6SS^-$ phenotypes conferred by the *mltE* mutation were complemented by the production of a wild-type copy of MltE (Fig. 3A and 3B). We then tested whether the activity of MltE is required for T6SS function. The crystal structure and the *in vitro* characterization of MltE revealed the importance of a glutamate residue, Glu-64, in the catalytic reaction [71,72]. Although the $MltE^{E64Q}$ catalytic inactive mutant was produced at levels comparable to wild-type MltE, cells producing $MltE^{E64Q}$ were unable to release Hcp and to provide a T6SS-dependent competitive advantage against *E. coli* K-12 (Fig. 3A and 3B). Taken together, these results demonstrate that the assembly of the EAEC Sci-1 T6SS requires the activity of the MltE lytic transglycosylase.

MltE is recruited and activated by TssM.

A number of LTGs, including that associated with T3SS, T4SS and flagella, have been shown to interact with machine components to facilitate local peptidoglycan degradation at the site of assembly [11,16,22]. Based on the results presented above, we hypothesized that MltE should be recruited to the T6SS apparatus. MltE being an outer-membrane lipoprotein facing the periplasm [73], we tested the interaction of a soluble form of MltE, $_{S}$MltE, with the T6SS subunits or domains exposed in the periplasm. These include the soluble fragment of TssJ, the periplasmic domains of the TssM (TssM$_{P}$) and TagL (TagL$_{P}$) proteins [30,58,60,63,64], as well as VgrG, which is proposed to fit inside the TssJLM complex channel at rest [30]. Bacterial two-hybrid analyses demonstrated that $_{S}$MltE interacts with the TssM periplasmic domain (Fig. 4A-B). This interaction is specific as $_{S}$MltE does not interact with the other T6SS subunits tested, and TssM$_{P}$ does not interact with the seven other LTGs. The interaction of TssM$_{P}$ with the full-length MltE lipoprotein was further confirmed by co-immune-precipitation into the heterologous host *E. coli* K-12 (Fig. 4C). These results define that MltE is recruited to the T6SS apparatus by binding directly to the TssM periplasmic region. The bacterial two-hybrid assay also showed that the $_{S}$MltE^{E64Q} variant interacts with TssM$_{P}$, demonstrating that this mutation does not interfere with MltE recruitment to TssM$_{P}$ (Fig. 4B). The TssM periplasmic region could be segmented into three sub-domains: sub-domains 1 and 2 (amino-acids 386-973) correspond to a region predicted to be essentially α-helical, and are followed by the C-terminal sub-domain 3 (amino-acids 974-1129) that folds as a β-sandwich-like structure [30]. Co-immune-precipitations using two variants encompassing these regions (TssM$_{386\text{-}973}$ and TssM$_{972\text{-}1129}$) revealed that MltE binds to the α-helical sub-domains 1+2 (Fig. 4C).

MltE is a non-processive *endo*-transglycosylase, which is considered to have a relatively low peptidoglycan hydrolase activity *in vivo* compared to other LTGs [73]. Indeed, peptidoglycan hydrolysis assays showed that purified soluble form of MltE, $_{S}$MltE, is significantly less active compared to lysozyme (Fig. 5A and 5B; initial rate of $_{S}$MltE= 0.45×10^{-3} AU/min/nmol). However, the activity of the T3SS-associated EtgA protein, has been shown to be modulated via its interaction with the T3SS rod component EscI to avoid unspecific peptidoglycan lysis [22]. We therefore tested whether $_{S}$MltE is activated once bound to TssM$_{P}$. Figures 5A and 5B show that incubation of $_{S}$MltE with TssM$_{P}$ stimulated the activity of $_{S}$MltE 7-fold (initial rate of $_{S}$MltE in presence of TssM$_{P}$= 3.15×10^{-3} AU/min/nmol).

Control experiments showed that $TssM_P$, the $_SMltE^{E64Q}$:$TssM_P$ complex or the $_SMltE$:$TssM_P$ complex in presence of Bulgecin A, have no significant activity (Fig. 5A and 5B).

MltE is required for oligomerisation of the TssM protein

The assembly of the T6SS is an ordered process in which the different subunits of the apparatus are sequentially recruited to the site of assembly. The assembly starts with the initial positioning of the TssJ lipoprotein and progresses by the addition of TssM and TssL, and the polymerization of TssJLM complexes to yield the membrane complex [30]. The cytoplasmic TssA protein then binds to the TssJM or TssJLM complex and recruits the baseplate, prior to tail polymerization [56,65,74]. To define at which stage of this biogenesis pathway the activity of MltE is necessary, we first assayed the TssJ-TssM and TssL-TssM interactions in the WT strain and its isogenic Δ*mltE* mutant. As previously published [64], TssJ and TssL co-precipitates with TssM. Figures 6A and 6B respectively show that TssJ-TssM and TssL-TssM interactions are not affected by the absence of MltE. The latter stages of T6SS membrane complex biogenesis is the polymerization of the TssJLM complex [30]. The multimerization of TssM and its complexes with TssJ and TssL could be visualized in wild-type cells after *in vivo* chemical cross-linking using bis-(sulfosuccinimidyl)-suberate (BS^3) (Fig. 6C). Although TssJM and TssML complexes are still assembled in Δ*mltE* cells or Δ*mltE* cells producing the $MltE^{E64Q}$ catalytic MltE mutant, no cross-linked TssM-TssM species were observed in these cells (Fig. 6C). Assembled TssJLM complexes can be observed directly in cells using a chromosomal fusion between TssM and a fluorescent reporter such as GFP [30]. Fluorescence microscopy recordings show that $_{GFP}$TssM forms fluorescent clusters at the cell periphery in wild-type cells (Fig. 6D). However, no focus was observable in Δ*mltE* cells or Δ*mltE* cells producing $MltE^{E64Q}$ (Fig. 6D). Taken together, these results suggest that local peptidoglycan hydrolysis by MltE is not required for formation of TssJLM hetero-trimers but rather is necessary for assembly of the TssJLM core complex.

Concluding remarks

In this work, we observed that treatment of EAEC cells with the LTG inhibitor bulgecin A prevents assembly of the Sci-1 T6SS. Systematic deletion of genes encoding LTG or putative LTG coupled to phenotypic assays demonstrated that the housekeeping MltE LTG is required

for Sci-1 T6SS function, as Hcp release in the culture supernatant was abolished in Δ*mltE* cells. In addition, Δ*mltE* cells presented a decreased T6SS-dependent antagonist activity against *E. coli* K-12. The EAEC strain used in this study, 17-2, encodes a second T6SS, Sci-2 that belongs to the T6SS-3 family [75]. No dedicated LTG is encoded within this cluster, and it will be thus interesting to define whether MltE - or an another host LTG - is required for the assembly of the Sci-2 T6SS.

We further showed that MltE is recruited to the site of assembly of the T6SS membrane complex by interacting with the α-domains 1 and 2 of the TssM periplasmic region. In addition, we showed that the presence of the periplasmic domain of TssM stimulates the LTG activity of MltE 7-fold *in vitro*. These results are comparable to the enteropathogenic *E. coli* EscI T3SS rod component that binds and stimulates the EtgA LTG or the. EtgA is a specialized LTG, encoded and co-regulated with the T3SS gene cluster [21,22,76], a situation that is common in cell-envelope spanning machines such as flagella, Type IV pili, T3SS or T4SS [3,5]. By contrast, with few exceptions [67], no peptidoglycan hydrolase is encoded within T6SS gene clusters. Therefore, assembly of the T6SS membrane complex requires hijacking of an host LTG to locally rearrange the cell wall. The *mltE* gene is also present in *E. coli* K-12 strains lacking T6SS, in which it participates to peptidoglycan homeostasis [10,73]. The EAEC Sci-1 T6SS has therefore re-routed MltE for its own assembly. However, the observation that T6SS gene clusters have been horizontally transferred between species suggests that each strain may have domesticated different host LTG. Another example of domestication of non-specialized LTG is the recruitment of MltD to anchor the *Helicobacter pylori* flagellum [77].

The recruitment of MltE by TssM therefore spatially controls the activity of MltE at close proximity to the site of assembly of the T6SS. Interestingly, MltE has a relatively weak activity on *E. coli* peptidoglycan compared to other LTGs [73]. However, Fibriansah *et al.* noted that MltE is more active on the peptidoglycan of *Micrococcus luteus*, which differs from that of *E. coli* by the nature of the peptide stems. They proposed that MltE activity either requires the activity of an amidase to cleave the peptidoglycan peptide moieties or that its conformation is modulated by protein partners [72]. The coordinated action of amidases and LTGs has been documented, notably during sporulation in *Bacillus subtilis* [78]. Although it would be interesting to test whether amidases are required for the assembly of the T6SS, the observation that TssM enhances the activity of MltE *in vitro* suggests that TssM helps MltE to

bypass the presence of peptide stems. TssM might displace the peptide stem to avoid steric hindrance and to increase accessibility of MltE to the glycan strand, or might induce a conformational change in MltE hence increasing its affinity for its substrate.

Our results also defined that MltE is required for the late stages of the assembly of the T6SS membrane complex (Fig. 7). The biogenesis of the T6SS membrane complex begins with the positioning of the TssJ outer membrane lipoprotein (Fig. 7a) and the recruitment of (i) TssM and (ii) TssL (Fig. 7b-c) prior to multimerization (Fig. 7d) [30]. The assembled TssJLM membrane complex is constituted of five dimers of TssJLM heterotrimeric complexes (Fig. 7d) [30]. We showed that the absence of MltE does not interfere with the interaction between TssJ and TssM, as well as between TssM and TssL. However, we did not detect TssM dimers in Δ*mltE* cells or in cells producing a catalically-inactive MltE LTG. We therefore propose that MltE is recruited to TssM prior to multimerization (Fig. 7). This hypothesis means that the monomeric periplasmic domain of TssM can cross the cell wall to interact with TssJ, and that local rearrangement of the peptidoglycan is necessary for the polymerization of TssJLM hetero-trimers.

Taken together, our results provide evidence that the EAEC Sci-1 T6SS has domesticated an endoneous LTG to allow the proper assembly and insertion of the cell-spanning complex.

Materials and Methods

Bacterial strains, growth conditions and chemicals

The strains used in this study are listed in Table EV1. *Escherichia coli* K-12 strains DH5α, W3110, BTH101 and BL21(DE3)/MC1061 were used for cloning procedures, co-immune-precipitation, bacterial two-hybrid and protein purification respectively. Enteroaggregative *E. coli* (EAEC) strains used in this work are isogenic derivatives of the wild-type O3:H2 17-2 strain. *E. coli* K-12 and EAEC cells were routinely grown in LB broth at 37°C, with aeration. For induction of the *sci-1* T6SS gene cluster, cells were grown in Sci-1-inducing medium (SIM: M9 minimal medium supplemented with glycerol (0.2%), vitamin B1 (1 µg/mL), casaminoacids (40 µg/mL), LB (10% v/v)) [79]. Plasmids and mutations were maintained by the addition of ampicillin (100 µg/mL for K-12, 200 µg/mL for EAEC), kanamycin (50 µg/mL for K-12, 50 µg/mL for chromosomal insertion on EAEC, 100 µg/mL for plasmid-bearing EAEC) or chloramphenicol (40 µg/mL). Gene expression was induced by the

addition of iso-propyl-β-D-thio-galactopyranoside (IPTG, Sigma-Aldrich, 0.2 mM for 1 hour), L-arabinose (Sigma-Aldrich; 0.005% for 0.5 hour for complementation assays, 0.2% for 1 hour for co-immuno-precipitation) or anhydrotetracyclin (AHT; IBA Technologies; 0.2 µg/mL for 45 min). Bulgecin A (a kind gift of Mathilde Bonis and Ivo G. Boneca (Institut Pasteur Paris)) was used at 50 µg/mL or 100 µg/mL for *in vitro* or *in vivo* inhibition experiments respectively.

Strain construction

Deletions of genes *mltA* (EC042_3012, gene accession identifier (GI): 284922752), *mltB* (EC042_2894, GI: 284922637), *mltC* (EC042_3170, GI: 284922906), *mltD* (EC042_0224, GI: 284920001), *mltE* (EC042_1244, GI: 284920999), *slt70* (EC042_4889, GI: 284924571), EC042_2762 (GI: 284922508) and *etgA* (EC042_3052, GI: 284922791) were engineered on the EAEC 17-2 chromosome using the modified one-step inactivation procedure [80] using λ red recombinase expressed from pKOBEG [81] as previously described [63]. The *mltE* gene was deleted from the 17-2 strain producing the $_{GFP}$TssM fusion protein expressed from the chromosomal native locus [30] using the same procedure. The kanamycine cassette from plasmid pKD4 [80] was amplified with oligonucleotides carrying ~ 50-nucleotide extensions homologous to regions adjacent to the target gene (custom primers, synthesized by Eurogentec, are listed in Table EV1). The Polymerase Chain Reaction (PCR) product was column purified (PCR and Gel Clean up, Promega) and electroporated into competent cells. Kanamycin resistant clones were selected and the insertion of the kanamycin cassette at the targeted site was verified by PCR. The kanamycin cassette was then excised using plasmid pCP20 [80] and the final strain was verified by PCR.

Plasmid construction

PCR were performed with a Biometra thermocycler, using the Pfu Turbo DNA polymerase (Stratagene; La Jolla, CA). Plasmids and oligonucleotides are listed in Table EV1. Constructions of pOK-Hcp$_{HA}$, pUC-Hcp$_{FLAG}$, pIBA-TssM$_{FL}$, pIBA-TssM$_{P}$, pMS-TssJ$_{HA}$ and pETG20A-TssM$_{P}$ have been previously described [60,63,64]. Plasmids pBADnLIC-sMltE and pBADnLIC-sMltE-E64Q have been previously described [72] and have been kindly provided by Andy-Mark Thunnissen (University of Groningen, The Netherlands). All pASK-IBA4 and bacterial two-hybrid vectors and the pBAD-MltE$_{V}$ plasmid, encoding the C-terminally VSV-G-tagged full-length MltE protein under the control of the arabinose promoter (in the pBAD33 vector), have been constructed by restriction-free cloning [82]. Briefly, the gene of interest fused to 5' and 3'-extensions annealing to the target vector was amplified and used as oligonucleotides for a second PCR using the target vector as template. The E64Q point mutation was inserted into pBAD-MltE$_{V}$ and pT18-MltE by site-directed mutagenesis

using complementary oligonucleotides bearing the desired mutation. All constructs have been verified by PCR and DNA sequencing (MWG).

T6SS phenotypic assays and $_{GFP}$TssM fluorescence microscopy recordings

Hcp release and anti-bacterial competition assays were performed as previously described [63,70]. For the Hcp release assay with bulgecin A treatment, the experiment was performed in a Δ*tssM* strain carrying plasmid pASK-IBA37-TssM, allowing AHT-dependent inducible expression of the *tssM* gene and producing HA-tagged Hcp. Cells were grown in SIM until A_{600} ~ 0.4 and treated - or not - with bulgecin A (100 µM). After 40 min, *tssM* expression was induced by the addition of AHT and the culture was further grown for 45 minutes. Cell pellets and supernatants were fractionated by centrifugation. The final supernatant fraction samples were obtained by filtration on 0.25 µM-PES membranes and TCA precipitation as previously published [63]. Controls were performed to verify that bulgecin A treatment did not interfere with TssM production. Controls for cell lysis were performed by immuno-detecting the periplasmic TolB protein. For treatment of cells with pre-assembled TssJLM complexes, wild-type 17-2 cells producing HA-tagged Hcp were grown in SIM to A_{600} ~ 0.5, and the cells and supernatant fractions were separated as described above. Cells were washed in SIM and resuspended in SIM supplemented- or not - with bulgecin A (100 µM). After further growth for 45 min, cells and supernatant fractions were separated as described above. Fluorescence microscopy recordings were performed as previously published [30]. All experiments have been done at least in duplicate and a representative result is shown. Statistical analysis of anti-bacterial competition assays was performed by Student's *t*-test. Significant differences were defined as $p < 0.05$ (*), $p < 0.01$ (**), and $p < 0.001$ (***).

Protein production and purification

The periplasmic domain of TssM was purified from *E. coli* BL21(DE3) cells carrying the pETG20A-TssM$_P$ plasmid and the native protein was obtained atfer cleavage of the Thioredoxin-6×His N-terminal extension by the tobacco etch virus (TEV) protease, as previously published [64]. The soluble MltE protein and its E64Q variant were purified from *E. coli* MC1061 cells carrying the pBADnLIC-sMltE or pBADnLIC-sMltE-E64Q vector as previously published [72].

Peptidoglycan hydrolysis assays

Preparation of the peptidoglycan fraction. The peptidoglycan fraction from the JE5505 *lpp* strain was prepared as previously published [83], resuspended in phosphate-buffered saline and treated with 200 µg/mL amylase (Sigma-Aldrich) for 2 hours at 37°C. *Remazol brilliant blue assay.* This protocol for the peptidoglycan hydrolysis assay has been modified from a published protocol [84]. The purified

peptidoglycan was washed with distilled water, resuspended in 200 mM NaOH and labeled with 25 mM Remazol brilliant blue (RBB, Sigma-Aldrich) for 14 hours at 37°C, and washed four times with distilled water. RBB-labeled peptidoglycan was incubated with the 50 µg of protein of interest for 30 min or 4 hours in PBS buffer, and the reaction was quenched by the addition of 50 µg/mL Bulgecin A. After ultra-centrifugation for 40 min at 68,000×*g*, the absorbance of the supernatant was measured at 595 nm. *Peptidoglycan turbidity assay*. This peptidoglycan hydrolysis assay has been performed as previously published [72] using a suspension of 0.25 mg/mL of purified *Micrococcus luteus* peptidoglycan (Sigma-Aldrich) in MES 50 mM pH6.0, NaCl 200 mM (A_{600}=0.57 ± 0.04). The turbidity at 600 nm was measured every 20 minutes after addition of 50 µg (~2.48 nmol) of $_{S}$MltE. For experiments in presence of TssM$_{P}$, a 1:2 ($_{S}$MltE:TssM$_{P}$) molar ratio have been used. The initial rate was measured as the slope of the initial linear curve (expressed in absorbance units/min/nmol). For all peptidoglycan hydrolysis assays, controls were performed with buffer, lysozyme or in presence of 50 µg/mL Bulgecin A. The assays have been performed in triplicate and a representative experiment is shown.

Bacterial two-hybrid assay

The adenylate cyclase-based bacterial two-hybrid technique [85] was used as previously published [86]. Briefly, the proteins to be tested were fused to the isolated T18 and T25 catalytic domains of the *Bordetella* adenylate cyclase. After introduction of the two plasmids producing the fusion proteins into the reporter BTH101 strain, plates were incubated at 30°C for 24 hours. Three independent colonies for each transformation were inoculated into 600 µL of LB medium supplemented with ampicillin, kanamycin and IPTG (0.5 mM). After overnight growth at 30°C, 10 µL of each culture were dropped onto LB plates supplemented with ampicillin, kanamycin, IPTG and 5-bromo-4-chloro-3-indolyl-β-D-galactopyranoside (X-Gal) and incubated for 16 hours at 30 °C. Controls include interaction assays with TolB and Pal, two protein partners unrelated to the T6SS. The experiments were done at least in triplicate and a representative result is shown.

Co-immune-precipitation

10^{11} exponentially growing cells producing the proteins of interest were harvested, and resuspended in buffer TN (Tris-HCl 20 mM pH8.0, NaCl 100 mM) supplemented with protease inhibitors (Complete, Roche), lysozyme (100 µg/mL) and DNase (100 µg/mL) and broken by three passages at the French press (1000 psi). Unbroken cells were discarded by centrifugation for 15 min at 3,000×*g* and the total cell extract was mixed with an equal volume of 2×CellLytic™ B Cell Lysis reagent (Sigma-Aldrich) and incubated for 1 hour with strong shaking. The insoluble material was discarded by centrifugation for 45 min at 60,000×*g* and the supernatant from 2×10^{10} cells was incubated overnight at 4°C with anti-FLAG M2 affinity beads (Sigma-Aldrich). Beads were then washed three times with

1×CellLytic™ in buffer TN. The total extract and immunoprecipitated material were resuspended and boiled in Laemmli loading buffer prior to analyses by SDS-PAGE and immunoblotting. The experiments were done in triplicate and a representative result is shown.

***In vivo* BS3 cross-linking assay**

2×10^9 exponentially growing cells were harvested, washed with sodium phosphate (SP) buffer (NaH_2PO_4/Na_2HPO_4 10 mM pH7.4), resuspended in 1 mL of SP supplemented with 0.5 mM bis (3-sulfo-N-hydroxy-succinimide ester) suberate (BS^3; Sigma-Aldrich). After incubation at room temperature for 25 min, the cross-linking reaction was quenched by the addition of Tris-HCl pH8.0 (100 mM final concentration). Cross-linked cells were resuspended and boiled in non-reducing Laemmli loading buffer prior to analyses by SDS-PAGE and immunoblotting. The experiments were done in triplicate and a representative result is shown.

Miscellaneous

For Western-blot analyses, cell extracts or precipitated proteins were resuspended in Laemmli buffer and boiled for 10 min. Proteins were separated by SDS-PAGE and transferred onto nitrocellulose membranes. Immunoblots were probed with anti-VSV-G (clone P5D4, Sigma-Aldrich), anti-FLAG (clone M2, Sigma-Aldrich), anti-HA (clone HA-7, Sigma-Aldrich) monoclonal antibodies, or anti-TolB polyclonal antibodies (laboratory collection) and anti-rabbit or anti-mouse secondary antibodies coupled to the alkaline phosphatase. Immunostaining was achieved in sodium phosphate buffer (pH9.0) supplemented with $MgCl_2$ 10mM, 5-bromo-4-chloro-3-indolyl-phosphate 40 µg/mL and nitro-blue tetrazolium chloride 40 µg/mL.

References

1. Costa TR, Felisberto-Rodrigues C, Meir A, Prevost MS, Redzej A, Trokter M, Waksman G (2015) Secretion systems in Gram-negative bacteria: structural and mechanistic insights. *Nat Rev Microbiol* 13: 343-359

2. Demchick P, Koch AL (1996) The permeability of the wall fabric of *Escherichia coli* and *Bacillus subtilis*. *J Bacteriol* 178: 768-773

3. Koraimann G (2003) Lytic transglycosylases in macromolecular transport systems of Gram-negative bacteria. *Cell Mol Life Sci* 60: 2371-2388

4. Zahrl D, Wagner M, Bischof K, Bayer M, Zavecz B, Beranek A, Ruckenstuhl C, Zarfel GE, Koraimann G (2005) Peptidoglycan degradation by specialized lytic transglycosylases associated with type III and type IV secretion systems. *Microbiology* 151: 3455-3467.

5. Scheurwater EM, Burrows LL (2011) Maintaining network security: how macromolecular structures cross the peptidoglycan layer. *FEMS Microbiol Lett* 318: 1-9

6. Höltje JV (1996) Lytic transglycosylases. *EXS* 75: 425-429

7. Scheurwater E, Reid CW, Clarke AJ (2008) Lytic transglycosylases: bacterial space-making autolysins. *Int J Biochem Cell Biol* 40: 586-591

8. Vollmer W, Joris B, Charlier P, Foster S (2008) Bacterial peptidoglycan (murein) hydrolases. *FEMS Microbiol Rev* 32: 259-286

9. Uehara T, Bernhardt TG (2011) More than just lysins: peptidoglycan hydrolases tailor the cell wall. *Curr Opin Microbiol* 14: 698-703

10. van Heijenoort J (2011) Peptidoglycan hydrolases of *Escherichia coli*. *Microbiol Mol Biol Rev* 75: 636-663

11. de la Mora J, Ballado T, González-Pedrajo B, Camarena L, Dreyfus G (2007) The flagellar muramidase from the photosynthetic bacterium *Rhodobacter sphaeroides*. *J Bacteriol* 189: 7998-8004

12. de la Mora J, Osorio-Valeriano M, González-Pedrajo B, Ballado T, Camarena L, Dreyfus G (2012) The C terminus of the flagellar muramidase SltF modulates the interaction with FlgJ in *Rhodobacter sphaeroides*. *J Bacteriol* 194: 4513-4520

13. Viollier PH, Shapiro L (2003) A lytic transglycosylase homologue, PleA, is required for the assembly of pili and the flagellum at the *Caulobacter crescentus* cell pole. *Mol Microbiol* 49: 331-345

14. Mushegian AR, Fullner KJ, Koonin EV, Nester EW (1996) A family of lysozyme-like virulence factors in bacterial pathogens of plants and animals. *Proc Natl Acad Sci USA* 93: 7321-7326

15. Ward DV, Draper O, Zupan JR, Zambryski PC (2002) Peptide linkage mapping of the *Agrobacterium tumefaciens* vir-encoded type IV secretion system reveals protein subassemblies. *Proc Natl Acad Sci USA* 99: 11493-11500

16. Höppner C, Carle A, Sivanesan D, Hoeppner S, Baron C (2005) The putative lytic transglycosylase VirB1 from *Brucella suis* interacts with the type IV secretion system core components VirB8, VirB9 and VirB11. *Microbiology* 151: 3469-3482

17. Kohler PL, Hamilton HL, Cloud-Hansen K, Dillard JP (2007) AtlA functions as a peptidoglycan lytic transglycosylase in the Neisseria gonorrhoeae type IV secretion system. *J Bacteriol* 189: 5421-5428

18. Zhong Q, Shao S, Mu R, Wang H, Huang S, Han J, Huang H, Tian S (2011) Characterization of peptidoglycan hydrolase in Cag pathogenicity island of *Helicobacter pylori*. *Mol Biol Rep* 38: 503-509

19. Guglielmetti S, Balzaretti S, Taverniti V, Miriani M, Milani C, Scarafoni A, Corona S, Ciranna A, Arioli S, Santala V, *et al* (2014) TgaA, a VirB1-like component belonging to a putative type IV secretion system of *Bifidobacterium bifidum* MIMBb75. *Appl Environ Microbiol* 80: 5161-5169

20. Creasey EA, Delahay RM, Daniell SJ, Frankel G (2003) Yeast two-hybrid system survey of interactions between LEE-encoded proteins of enteropathogenic *Escherichia coli*. *Microbiology* 149: 2093-2106

21. García-Gómez E, Espinosa N, de la Mora J, Dreyfus G, González-Pedrajo B (2011) The muramidase EtgA from enteropathogenic *Escherichia coli* is required for efficient type III secretion. *Microbiology* 157: 1145-1160

22. Burkinshaw BJ, Deng W, Lameignère E, Wasney GA, Zhu H, Worrall LJ, Finlay BB, Strynadka NC (2015) Structural analysis of a specialized type III secretion system peptidoglycan-cleaving enzyme. *J Biol Chem* 290: 10406-10417

23. Nambu T, Minamino T, Macnab RM, Kutsukake K (1999) Peptidoglycan-hydrolyzing activity of the FlgJ protein, essential for flagellar rod formation in *Salmonella typhimurium*. *J Bacteriol* 181: 1555-1561

24. Hirano T, Minamino T, Macnab RM (2001) The role in flagellar rod assembly of the N-terminal domain of *Salmonella* FlgJ, a flagellum-specific muramidase. *J Mol Biol* 312: 359-369

25. Nambu T, Inagaki Y, Kutsukake K (2006) Plasticity of the domain structure in FlgJ, a bacterial protein involved in flagellar rod formation. *Genes Genet Syst* 81: 381-389

26. Hashimoto W, Ochiai A, Momma K, Itoh T, Mikami B, Maruyama Y, Murata K (2009) Crystal structure of the glycosidase family 73 peptidoglycan hydrolase FlgJ. *Biochem Biophys Res Commun* 381: 16-21

27. Herlihey FA, Moynihan PJ, Clarke AJ (2014) The essential protein for bacterial flagella formation FlgJ functions as a β-N-acetylglucosaminidase. *J Biol Chem* 289: 31029-31042

28. Rambow-Larsen AA, Weiss AA (2002) The PtlE protein of *Bordetella pertussis* has peptidoglycanase activity required for Ptl-mediated pertussis toxin secretion. *J Bacteriol* 184: 2863-2869

29. Herlihey FA, Osorio-Valeriano M, Dreyfus G, Clarke AJ (2016) Modulation of the lytic activity of the dedicated autolysin for flagellum formation SltF by flagellar rod proteins FlgB and FlgF. *J Bacteriol* 198: 1847-1856

30. Durand E, Nguyen VS, Zoued A, Logger L, Péhau-Arnaudet G, Aschtgen MS, Spinelli S, Desmyter A, Bardiaux B, Dujeancourt A *et al* (2015) Biogenesis and structure of a type VI secretion membrane core complex. *Nature* 523: 555-560

31. Bingle LE, Bailey CM, Pallen MJ (2008) Type VI secretion: a beginner's guide. *Curr Opin Microbiol* 11: 3-8

32. Cascales E (2008) The type VI secretion toolkit. *EMBO Rep* 9: 735-741

33. Silverman JM, Brunet YR, Cascales E, Mougous JD (2012) Structure and regulation of the type VI secretion system. *Annu Rev Microbiol* 66: 453-472

34. Kapitein N, Mogk A (2013) Deadly syringes: type VI secretion system activities in pathogenicity and interbacterial competition. *Curr Opin Microbiol* 16: 52-58

35. Coulthurst SJ (2013) The Type VI secretion system - a widespread and versatile cell targeting system. *Res Microbiol* 164: 640-654.

36. Russell AB, Peterson SB, Mougous JD (2014) Type VI secretion system effectors: poisons with a purpose. *Nat Rev Microbiol* 12: 137-148

37. Zoued A, Brunet YR, Durand E, Aschtgen MS, Logger L, Douzi B, Journet L, Cambillau C, Cascales E (2014) Architecture and assembly of the Type VI secretion system. *Biochim Biophys Acta* 1843: 1664-1673

38. Durand E, Cambillau C, Cascales E, Journet L (2014) VgrG, Tae, Tle, and beyond: the versatile arsenal of Type VI secretion effectors. *Trends Microbiol* 22: 498-507

39. Ho BT, Dong TG, Mekalanos JJ (2014) A view to a kill: the bacterial type VI secretion system. *Cell Host Microbe* 15: 9-21

40. Basler M (2015) Type VI secretion system: secretion by a contractile nanomachine. *Philos Trans R Soc Lond B Biol Sci* 370: 1679

41. Cianfanelli FR, Monlezun L, Coulthurst SJ (2016) Aim, Load, Fire: The Type VI secretion system, a bacterial nanoweapon. *Trends Microbiol* 24: 51-62

42. Hachani A, Wood TE, Filloux A (2016) Type VI secretion and anti-host effectors. *Curr Opin Microbiol* 29: 81-93

43. Bönemann G, Pietrosiuk A, Mogk A (2010) Tubules and donuts: a type VI secretion story. *Mol Microbiol* 76: 815-821

44. Cascales E, Cambillau C (2012) Structural biology of type VI secretion systems. *Philos Trans R Soc Lond B Biol Sci* 367: 1102-1111

45. Leiman PG, Shneider MM (2012) Contractile tail machines of bacteriophages. *Adv Exp Med Biol* 726: 93-114

46. Ballister ER, Lai AH, Zuckermann RN, Cheng Y, Mougous JD (2008) In vitro self-assembly of tailorable nanotubes from a simple protein building block. *Proc Natl Acad Sci USA* 105: 3733-3738

47. Leiman PG, Basler M, Ramagopal UA, Bonanno JB, Sauder JM, Pukatzki S, Burley SK, Almo SC, Mekalanos JJ (2009) Type VI secretion apparatus and phage tail-associated protein complexes share a common evolutionary origin. *Proc Natl Acad Sci USA* 106: 4154-4159

48. Brunet YR, Hénin J, Celia H, Cascales E (2014) Type VI secretion and bacteriophage tail tubes share a common assembly pathway. *EMBO Rep* 15: 315-321

49. Basler M, Pilhofer M, Henderson GP, Jensen GJ, Mekalanos JJ (2012) Type VI secretion requires a dynamic contractile phage tail-like structure. *Nature* 483: 182-186

50. Kudryashev M, Wang RY, Brackmann M, Scherer S, Maier T, Baker D, DiMaio F, Stahlberg H, Egelman EH, Basler M (2015) Structure of the type VI secretion system contractile sheath. *Cell* 160: 952-562

51. Shneider MM, Buth SA, Ho BT, Basler M, Mekalanos JJ, Leiman PG (2013) PAAR-repeat proteins sharpen and diversify the type VI secretion system spike. *Nature* 500: 350-353

52. LeRoux M, De Leon JA, Kuwada NJ, Russell AB, Pinto-Santini D, Hood RD, Agnello DM, Robertson SM, Wiggins PA, Mougous JD (2012) Quantitative single-cell characterization of bacterial interactions reveals type VI secretion is a double-edged sword. *Proc Natl Acad Sci USA* 109: 19804-19809

53. Basler M, Ho BT, Mekalanos JJ (2013) Tit-for-tat: type VI secretion system counterattack during bacterial cell-cell interactions. *Cell* 152: 884-894

54. Brunet YR, Espinosa L, Harchouni S, Mignot T, Cascales E (2013) Imaging type VI secretion-mediated bacterial killing. *Cell Rep* 3: 36-41

55. English G, Byron O, Cianfanelli FR, Prescott AR, Coulthurst SJ (2014) Biochemical analysis of TssK, a core component of the bacterial Type VI secretion system, reveals distinct oligomeric states of TssK and identifies a TssK-TssFG subcomplex. *Biochem J* 461: 291-304

56. Brunet YR, Zoued A, Boyer F, Douzi B, Cascales E (2015) The Type VI secretion TssEFGK-VgrG phage-like baseplate is recruited to the TssJLM membrane complex via multiple contacts and serves as assembly platform for tail tube/sheath polymerization. *PLoS Genet* 11: e1005545

57. Taylor NM, Prokhorov NS, Guerrero-Ferreira RC, Shneider MM, Browning C, Goldie KN, Stahlberg H, Leiman PG (2016) Structure of the T4 baseplate and its function in triggering sheath contraction. *Nature* 533: 346-352

58. Logger L, Aschtgen MS, Guérin M, Cascales E, Durand E. (2016) Molecular dissection of the interface between the Type VI secretion TssM cytoplasmic domain and the TssG baseplate component. *J Mol Biol*. 428: 4424-4437.

59. Zoued A, Cassaro CJ, Durand E, Douzi B, España AP, Cambillau C, Journet L, Cascales E. (2016) Structure-function analysis of the TssL cytoplasmic domain reveals a new interaction between the Type VI secretion baseplate and membrane complexes. *J Mol Biol.* 428: 4413-4423.

60. Aschtgen MS, Gavioli M, Dessen A, Lloubès R, Cascales E (2010) The SciZ protein anchors the enteroaggregative *Escherichia coli* Type VI secretion system to the cell wall. *Mol Microbiol* 75: 886-899

61. Aschtgen MS, Zoued A, Lloubès R, Journet L, Cascales E (2012) The C-tail anchored TssL subunit, an essential protein of the enteroaggregative *Escherichia coli* Sci-1 Type VI secretion system, is inserted by YidC. *Microbiologyopen* 1: 71-82

62. Ma LS, Lin JS, Lai EM (2009) An IcmF family protein, ImpLM, is an integral inner membrane protein interacting with ImpKL, and its walker a motif is required for type VI secretion system-mediated Hcp secretion in *Agrobacterium tumefaciens*. *J Bacteriol* 191: 4316-4329

63. Aschtgen MS, Bernard CS, de Bentzmann S, Lloubès R, Cascales E (2008) SciN is an outer membrane lipoprotein required for type VI secretion in enteroaggregative *Escherichia coli*. *J Bacteriol* 190: 7523-7531

64. Felisberto-Rodrigues C, Durand E, Aschtgen MS, Blangy S, Ortiz-Lombardia M, Douzi B, Cambillau C, Cascales E (2011) Towards a structural comprehension of bacterial type VI secretion systems: characterization of the TssJ-TssM complex of an *Escherichia coli* pathovar. *PLoS Pathog*. 7: e1002386

65. Zoued A, Durand E, Brunet YR, Spinelli S, Douzi B, Guzzo M, Flaugnatti N, Legrand P, Journet L, Fronzes R *et al* (2016) Priming and polymerization of a bacterial contractile tail structure. *Nature* 531: 59-63

66. Aschtgen MS, Thomas MS, Cascales E (2010) Anchoring the type VI secretion system to the peptidoglycan: TssL, TagL, TagP... what else? *Virulence* 1: 535-540

67. Weber BS, Hennon SW, Wright MS, Scott NE, de Berardinis V, Foster LJ, Ayala JA, Adams MD, Feldman MF. (2016) Genetic dissection of the Type VI secretion system in *Acinetobacter* and identification of a novel peptidoglycan hydrolase, TagX, required for its biogenesis. *MBio*. 7: e01253-16.

68. Imada A, Kintaka K, Nakao M, Shinagawa S (1982) Bulgecin, a bacterial metabolite which in concert with beta-lactam antibiotics causes bulge formation. *J Antibiot (Tokyo)* 35: 1400-1403

69. Thunnissen AM, Rozeboom HJ, Kalk KH, Dijkstra BW (1995) Structure of the 70-kDa soluble lytic transglycosylase complexed with bulgecin A. Implications for the enzymatic mechanism. *Biochemistry* 34: 12729-12737

70. Flaugnatti N, Le TT, Canaan S, Aschtgen MS, Nguyen VS, Blangy S, Kellenberger C, Roussel A, Cambillau C, Cascales E *et al* (2016) A phospholipase A1 antibacterial Type VI secretion effector interacts directly with the C-terminal domain of the VgrG spike protein for delivery. *Mol Microbiol* 99: 1099-1118

71. Artola-Recolons C, Carrasco-López C, Llarrull LI, Kumarasiri M, Lastochkin E, Martínez de Ilarduya I, Meindl K, Usón I, Mobashery S, Hermoso JA (2011) High-resolution crystal structure of MltE, an outer membrane-anchored endolytic peptidoglycan lytic transglycosylase from *Escherichia coli*. *Biochemistry* 50: 2384-2386

72. Fibriansah G, Gliubich FI, Thunnissen AM (2012) On the mechanism of peptidoglycan binding and cleavage by the endo-specific lytic transglycosylase MltE from *Escherichia coli*. *Biochemistry* 51: 9164-9177

73. Kraft AR, Templin MF, Höltje JV (1998) Membrane-bound lytic endotransglycosylase in *Escherichia coli*. *J Bacteriol* 180: 3441-3447

74. Gerc AJ, Diepold A, Trunk K, Porter M, Rickman C, Armitage JP, Stanley-Wall NR, Coulthurst SJ (2015) Visualization of the *Serratia* Type VI secretion system reveals unprovoked attacks and dynamic assembly. *Cell Rep* 12: 2131-2142

75. Journet L, Cascales E (2016) The Type VI secretion system in *Escherichia coli* and related species. *EcoSal Plus* 7: 1-19

76. Yu YC, Lin CN, Wang SH, Ng SC, Hu WS, Syu WJ (2010) A putative lytic transglycosylase tightly regulated and critical for the EHEC type three secretion. *J Biomed Sci* 17: 52

77. Roure S, Bonis M, Chaput C, Ecobichon C, Mattox A, Barrière C, Geldmacher N, Guadagnini S, Schmitt C, Prévost MC *et al* (2012) Peptidoglycan maturation enzymes affect flagellar functionality in bacteria. *Mol Microbiol* 86: 845-856

78. Morlot C, Uehara T, Marquis KA, Bernhardt TG, Rudner DZ (2010) A highly coordinated cell wall degradation machine governs spore morphogenesis in *Bacillus subtilis*. *Genes Dev* 24: 411-422

79. Brunet YR, Bernard CS, Gavioli M, Lloubès R, Cascales E (2011) An epigenetic switch involving overlapping Fur and DNA methylation optimizes expression of a type VI secretion gene cluster. *PLoS Genet* 7: e1002205

80. Datsenko KA, Wanner BL (2000) One-step inactivation of chromosomal genes in *Escherichia coli* K-12 using PCR products. *Proc Natl Acad Sci USA* 97: 6640-6645

81. Chaveroche MK, Ghigo JM, d'Enfert C (2000) A rapid method for efficient gene replacement in the filamentous fungus *Aspergillus nidulans*. *Nucleic Acids Res* 28: E97

82. van den Ent F, Löwe J (2006) RF cloning: a restriction-free method for inserting target genes into plasmids. *J Biochem Biophys Methods* 67: 67-74

83. Cascales E, Lloubès R (2004) Deletion analyses of the peptidoglycan-associated lipoprotein Pal reveals three independent binding sequences including a TolA box. *Mol Microbiol* 51: 873-885

84. Uehara T, Parzych KR, Dinh T, Bernhardt TG (2010) Daughter cell separation is controlled by cytokinetic ring-activated cell wall hydrolysis. *EMBO J* 29: 1412-1422

85. Karimova G, Pidoux J, Ullmann A, Ladant D (1998) A bacterial two-hybrid system based on a reconstituted signal transduction pathway. *Proc Natl Acad Sci USA* 95: 5752-5756

86. Battesti A, Bouveret E (2012) The bacterial two-hybrid system based on adenylate cyclase reconstitution in *Escherichia coli*. *Methods* 58: 325-334

87. Durand E, Zoued A, Spinelli S, Watson PJ, Aschtgen MS, Journet L, Cambillau C, Cascales E (2012) Structural characterization and oligomerization of the TssL protein, a component shared by bacterial type VI and type IVb secretion systems. *J Biol Chem* 287: 14157-14168

Acknowledgements

This work is dedicated to Odette Santin in loving memory. We thank Mathilde Bonis and Ivo Gomperts Boneca (Institut Pasteur, Paris, France) for providing Bulgecin A, Andy-Mark Thunnissen (University of Groningen, The Netherlands) for providing 6×His-tagged $_{S}$MltE-overexpressing plasmids and protocols for $_{S}$MltE peptidoglycan hydrolase activity, Laureen Logger for the recruitment of Yoann, Yannick R. Brunet for the identification of LTG genes in the EAEC genome, Laure Journet, Eric Durand, Abdelrahim Zoued, Laureen Logger, Laetitia Houot and Bérengère Ize for assistance and insightful discussions, Emmanuelle Bouveret for advices regarding the bacterial two-hybrid assay, Van Son Nguyen for providing purified TssM$_{P}$, Keith Dudley (Aix-Marseille Université) and the members of the Lloubès, Bouveret and Sturgis research groups for discussions, Isabelle Bringer, Annick Brun and Olivier Uderso for technical assistance, and Jean-Romé Uhne-Couch for encouragements. Work on the T6SS in E.C. laboratory is supported by the CNRS, the Aix-Marseille Université and grants from the Agence National de la Recherche (ANR-10-JCJC-1303-03 and ANR-14-CE14-0006-02). Part of this work has been performed in fulfillment of Y.S. Aix-Marseille Université BIO99 project.

Author contributions. Y.S. and E.C. designed the research and conceived the study; Y.S. and E.C. performed the experiments; E.C. wrote the manuscript.

Additional Information. Table EV1 lists the strains, plasmids and oligonucleotides used in this study is available. Correspondence and requests for material should be addressed to E.C.

Competing interests. The authors declare no competing financial interests.

Legend to Figures

Figure 1. The LTG inhibitor Bulgecin A prevents T6SS function.

A Hcp release assay. HA-tagged Hcp (Hcp_{HA}) release was assessed by separating cells (C) and cell-free culture supernatant (S) fractions from 10^9 wild-type (WT), Δ*tssM* cells or Δ*tssM* cells carrying the AHT-inducible FLAG-tagged *tssM*-borne plasmid (*tssM*$^+$) treated (bulgecin) or not (NT) with bulgecin A prior to *tssM* gene induction. Proteins were separated by 12.5%-acrylamide SDS-PAGE and the periplasmic TolB protein (control for cell lysis), Hcp_{HA} and $_{FL}$TssM were immunodetected using anti-TolB (middle panel), anti-HA (lower panel) and anti-FLAG (upper panel) antibodies. Molecular weight markers (in kDa) are indicated on the left. The experiment was performed in duplicate and a representative result is shown.

B Hcp release assay. HA-tagged Hcp (Hcp_{HA}) release was assessed by separating cells (C) and cell-free culture supernatant (S) fractions from 10^9 wild-type (WT) cells before washing cells (before wash) and after washing and growth (after wash) in absence (NT) or presence (bulgecin) of bulgecin A. Proteins were separated by 12.5%-acrylamide SDS-PAGE and the periplasmic TolB protein (control for cell lysis) and Hcp_{HA} were immunodetected using anti-TolB (upper panel) and anti-HA (lower panel) antibodies. Molecular weight markers (in kDa) are indicated on the left. The experiment was performed in duplicate and a representative result is shown.

Figure 2. The MltE LTG is required for T6SS function.

Hcp release assay. FLAG-tagged Hcp (Hcp_{FL}) release was assessed by separating cells (C) and cell-free culture supernatant (S) fractions from 10^9 cells of the indicated strains. Proteins were separated by 12.5%-acrylamide SDS-PAGE and TolB and Hcp_{FL} were immunodetected using anti-TolB (upper panel) and anti-FLAG (lower panel) antibodies. Molecular weight markers (in kDa) are indicated on the left. The experiment was performed in triplicate and a representative result is shown.

Figure 3. The MltE peptidoglycan hydrolase activity is required for T6SS function.

A Hcp release assay. FLAG-tagged Hcp (Hcp_{FL}) release was assessed by separating cells (C) and cell-free culture supernatant (S) fractions from 10^9 WT, Δ*mltE* cells or Δ*mltE* cells producing wild-type (*mltE*$^+$) or E64Q mutant (*mltE*^{E64Q}) VSV-G-tagged MltE ($MltE_V$) from arabinose-inducible plasmids. Proteins were separated by 12.5%-acrylamide SDS-PAGE and TolB, Hcp_{FL} and $MltE_V$ were immunodetected using anti-TolB (upper panel), anti-FLAG (middle panel) and anti-VSV-G (lower panel) antibodies, respectively. Molecular weight markers (in kDa) are

indicated on the left. The experiment was performed in triplicate and a representative result is shown.

B Anti-bacterial activity. *E. coli* K-12 prey cells (W3110 gfp^+, kan^R) were mixed with the indicated attacker cells, spotted onto Sci-1 inducing medium (SIM) agar plates and incubated for 4 hours at 37°C. The image of a representative bacterial spot and the average and standard deviation (n=3) of the relative fluorescence of the bacterial mixture (in arbitrary unit, AU) are shown in the upper graph. The number of recovered *E. coli* prey cells (counted on selective kanamycin medium) is indicated in the lower graph (in log10 of colony-forming unit (cfu)). The black, dark grey and light grey circles indicate values from three independent assays, and the average is indicated by the bar. The experiment was performed in triplicate and a representative result is shown. Asterisks indicate significant differences compared to the wild-type attacker strain (NS, non significant; ***, $p < 0.001$).

Figure 4. MltE interacts with the TssM periplasmic domain.

A-B Bacterial two-hybrid assay. BTH101 reporter cells producing the indicated proteins or domains fused to the T18 or T25 domain of the *Bordetella* adenylate cyclase were spotted on X-Gal indicator plates. The blue color of the colony reflects the interaction between the two proteins. TolB and Pal are two proteins known to interact but unrelated to the T6SS or the MltE proteins. The experiment was performed in triplicate and a representative result is shown.

C Co-immunoprecipitation assay. The solubilized lysates from 2×10^{10} *E. coli* K-12 W3110 cells co-producing the indicated FLAG-tagged $TssM_P$ variants (exported in the periplasm) and VSV-G-tagged MltE protein (Total, T) were subjected to immune precipitation on anti-FLAG-coupled agarose beads. The immunoprecipitated material (IP) was subjected to 12.5%-acrylamide SDS-PAGE and immunodetected with anti-FLAG (upper panel, TssM domains) and anti-VSV-G (lower panel, MltE) antibodies. Molecular weight markers (in kDa) are indicated on the left. The experiment was performed in triplicate and a representative result is shown.

Figure 5. $TssM_P$ increases MltE peptidoglycan hydrolase activity.

A Remazol brilliant blue assay. The absorbance of supernatants from the reaction containing purified and RBB-labelled *E. coli* peptidoglycan and the indicated protein (50 µg) were measured at λ=595 nm after incubation for 0.5 or 4 hours at 37°C. The results shown are the average and standard deviation from triplicate reactions (n=3). Asterisks indicate significant differences compared to the buffer (NS, non significant; **, $p < 0.01$; ***, $p < 0.001$). The supernatant of the reaction after 4 hours of incubation is shown on bottom.

B Peptidoglycan hydrolysis. The decrease of the absorbance of the *M. luteus* peptidoglycan suspension in presence of the indicated protein (50 µg) was measured at λ=600 nm at 37°C over time. The experiment was performed in triplicate and a representative result is shown.

Figure 6. MltE is required for TssM multimerization.

A-B Co-immunoprecipitation assay. The solubilized lysates from 2×10^{10} EAEC wild-type or Δ*mltE* cells producing FLAG-tagged TssM ($_{FL}$TssM) and/or HA-tagged TssJ (TssJ$_{HA}$, panel A) or TssL (TssL$_{HA}$, panel B) (Total, T) were subjected to immune precipitation on anti-FLAG-coupled agarose beads. The immunoprecipitated material (IP) was subjected to 12.5%-acrylamide SDS-PAGE and immunodetected with anti-FLAG (upper panel, TssM) and anti-HA (lower panel, TssJ or TssL) antibodies. Molecular weight markers (in kDa) are indicated on the left. The experiments were performed in triplicate and a representative result is shown.

C BS^3 cross-linking assay. 2×10^9 cells of the indicated strain producing FLAG-tagged TssM (with the exception of Δ*tssM* cells) were treated (+) or not (-) with the BS^3 cross-linker agent. After the cross-linking reaction, cells were boiled in Laemmli buffer and total proteins were subjected to 7%-acrylamide SDS-PAGE and immunodetected with anti-FLAG antibodies. The TssM protein ($_{FL}$TssM) and its complexes (*, TssM-TssJ; **, TssM-TssL) are indicated on the right as well as the TssM dimer (arrow). Molecular weight markers (in kDa) are indicated on the left. The experiment was performed in triplicate and a representative result is shown.

D Fluorescence microscopy. Recordings showing TssM localization using the chromosomally-encoded *sfGFP-tssM* fusion in wild-type (WT) or Δ*mltE* cells or Δ*mltE* cells producing the wild-type ($mltE^+$) or catalytic variant ($mltE^{E64Q}$) MltE protein. Scale bars are 1 µm. The experiment was performed in triplicate and a representative result is shown.

Figure 7. Schematic model of the assembly of the TssJLM complex.

Biogenesis of the TssJLM complex begins with the initial positioning of the TssJ outer membrane (OM) lipoprotein (a) and the sequential recruitment of the TssM (b) and TssL (c) inner membrane (IM) proteins. TssM binds to the TssJ lipoprotein via its C-terminal β-domain 3 (dark blue) and recruits the MltE LTG (green ball) via its α-domain 1+2 (light blue). The TssM-mediated activation of MltE creates localized degradation in the cell wall (PG) allowing polymerization of the TssJLM complex (d). The crystal and electron microscopy structures are shown (TssJ, PDB:3RX9 [64]; TssM$_P$-TssJ complex, PDB:4Y7O [30]; TssL cytoplasmic domain, PDB: 3U66 [87]; TssJLM complex, EMDB:2927 [30]).

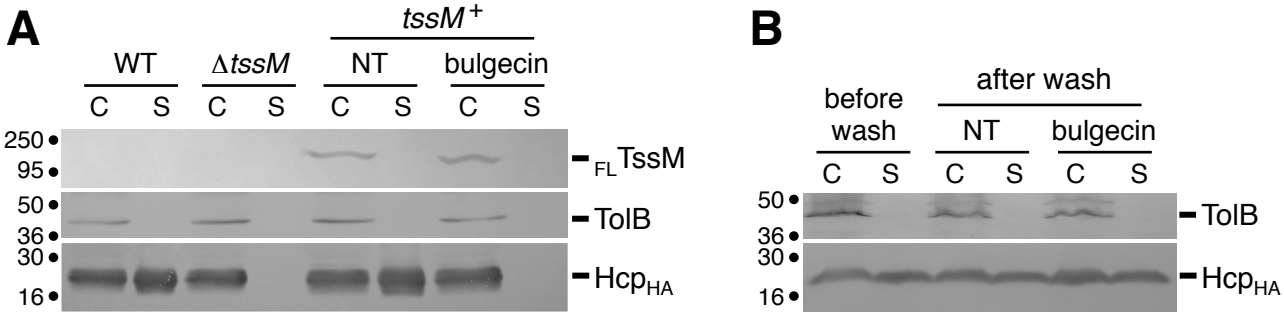

Santin et al. Figure 1

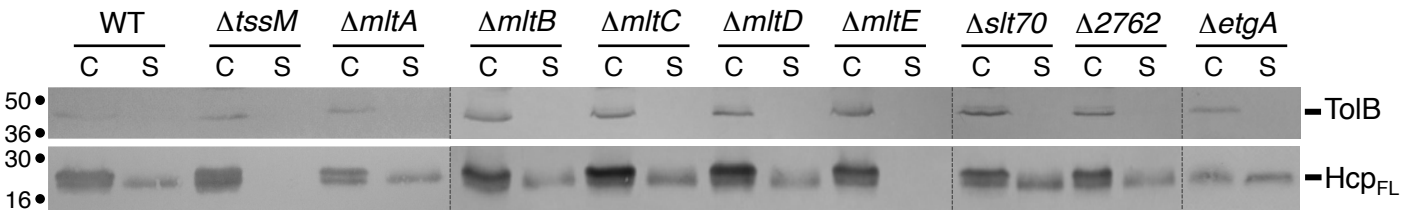

Santin et al. Figure 2

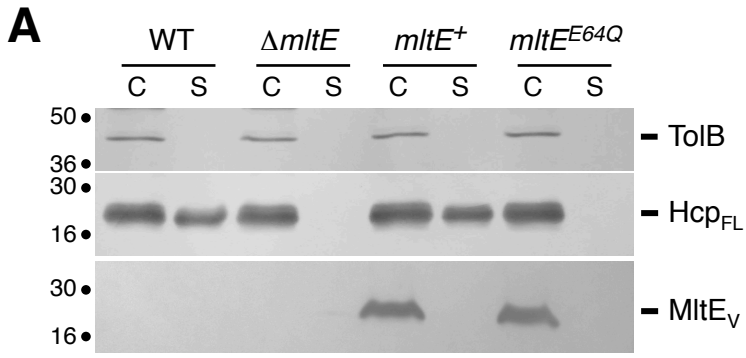

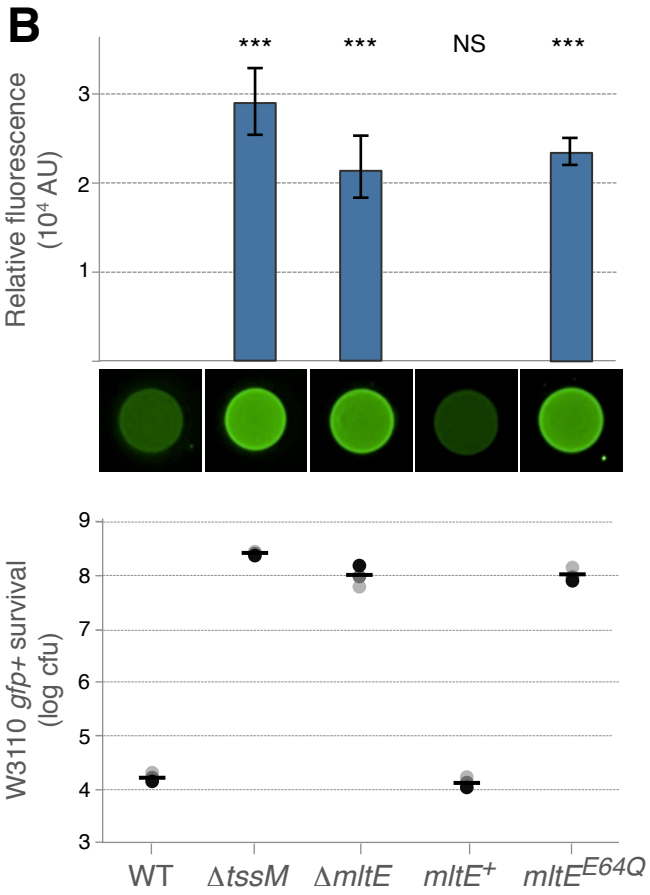

Santin et al. Figure 3

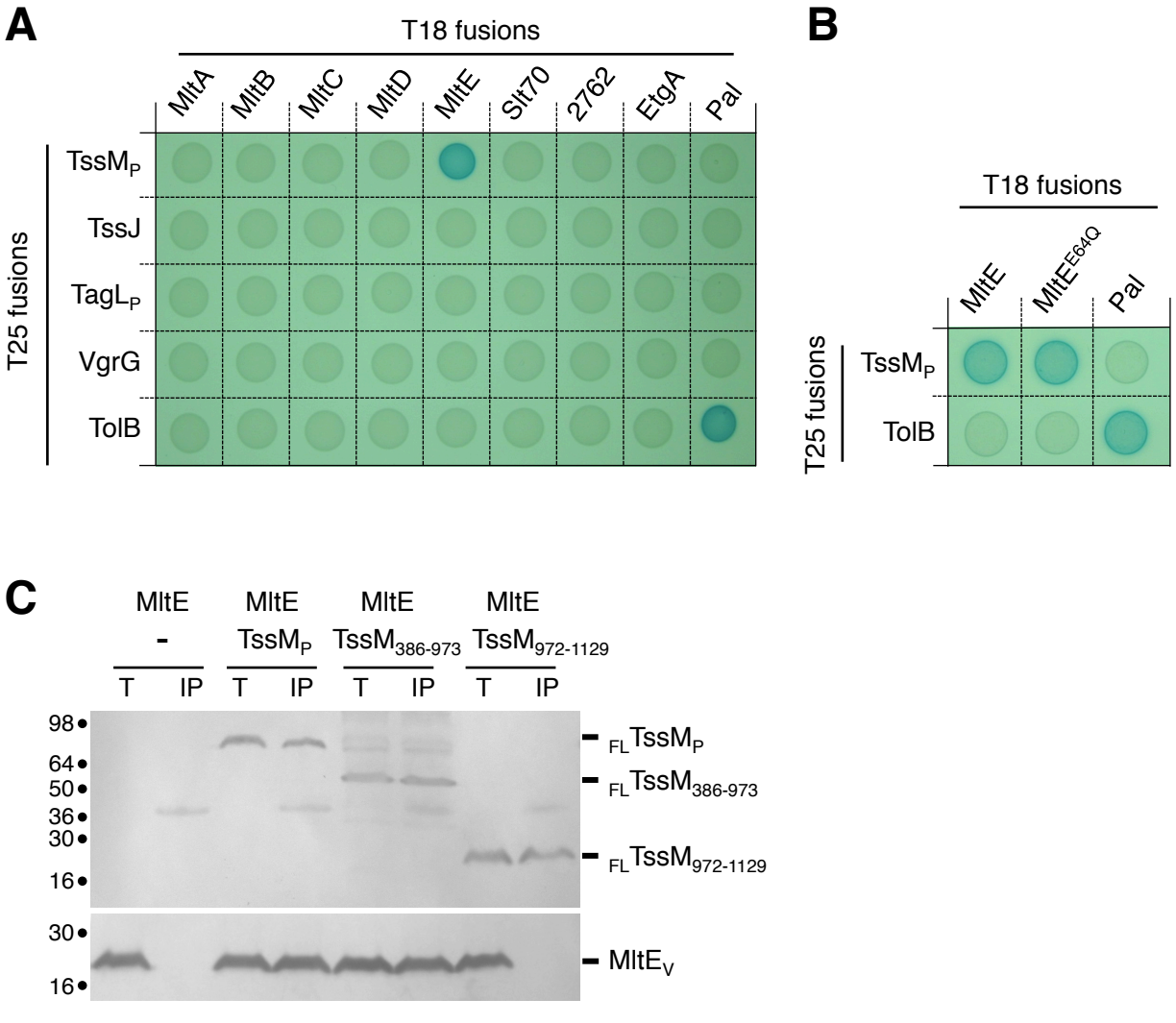

Santin et al. Figure 4

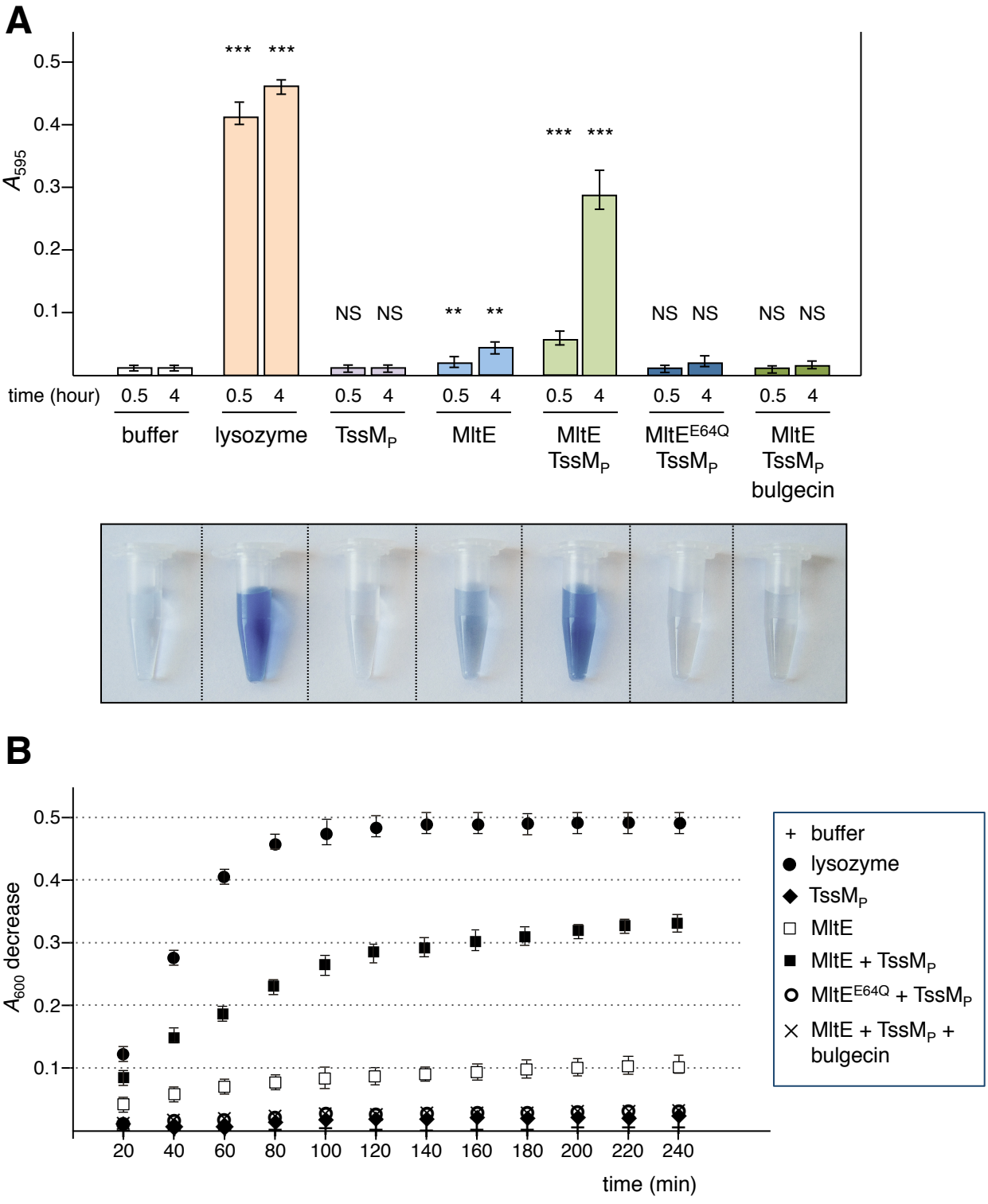

Santin et al. Figure 5

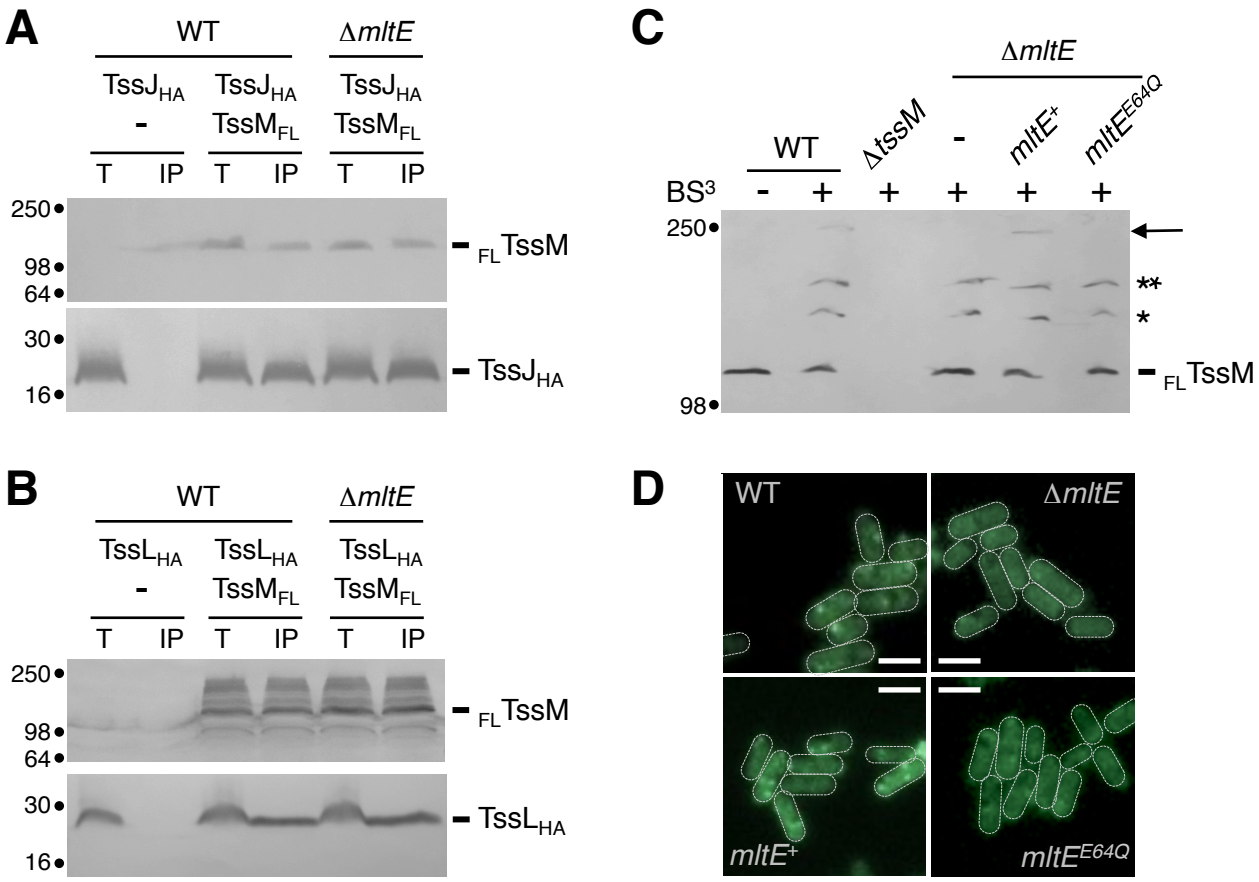

Santin et al. Figure 6

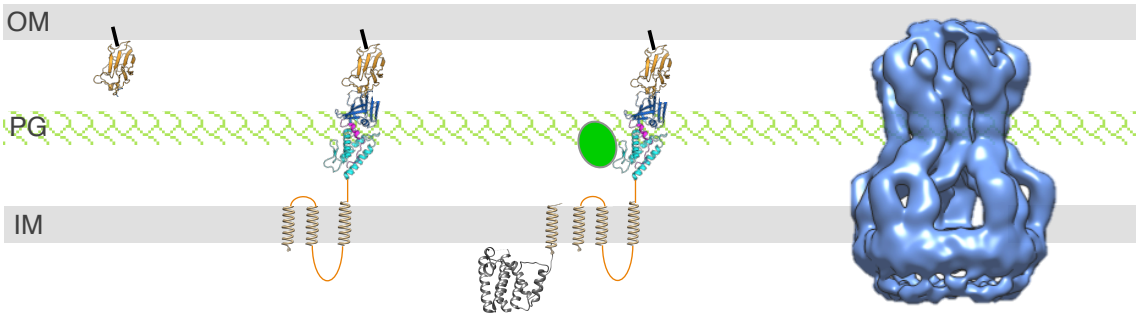

a.
TssJ
positioning

b.
TssM
recruitment

c.
MltE and TssL
recruitment

d.
Local degradation of
peptidoglycan and
TssJLM
polymerization

Santin et al. Figure 7

SUPPLEMENTAL DATA

Domestication of a housekeeping transglycosylase for assembly of a Type VI secretion system.

Y.G. Santin and E. Cascales

Supplemental Table S1. Strains, plasmids and oligonucleotides used in this study.

Strains

Strains	Description and genotype	Source
E. coli K-12		
DH5α	F-, Δ(*argF-lac*)U169, *phoA*, *supE44*, Δ(*lacZ*)M15, *relA*, *endA*, *thi*, *hsdR*	New England Biolabs
W3110	F-, lambda- IN(*rrnD-rrnE*)1 *rph*-1	Laboratory collection
BTH101	F-, *cya-99, araD139, galE15, galK16, rpsL1 (Str r), hsdR2, mcrA1, mcrB1.*	Karimova *et al.*, 2005
BL21(DE3)	F-, *fhuA2*, *lon*, *ompT*, *gal (λ int::(lacI::PlacUV5::T7 gene1)*, *dcm*, Δ*hsdS*	New England Biolabs
MC1061	F-, *araD139 Δ(ara-leu)*, *galE15*, *galK16*, Δ*(lac)X74*, *rpsL* (Str^R) *hsdR2 mcrAB1*	New England Biolabs
Enteroaggregative *E. coli*		
17-2	WT enteroaggregative *Escherichia coli*	Arlette Darfeuille-Michaud
17-2Δ*tssM*	17-2 deleted of the *tssM* gene of the *sci1* T6SS gene cluster	Aschtgen *et al.*, 2010
17-2Δ*mltA*	17-2 deleted of the *mltA* gene	This study
17-2Δ*mltB*	17-2 deleted of the *mltB* gene	This study
17-2Δ*mltC*	17-2 deleted of the *mltC* gene	This study
17-2Δ*mltD*	17-2 deleted of the *mltD* gene	This study
17-2Δ*mltE*	17-2 deleted of the *mltE* gene	This study
17-2Δ*slt70*	17-2 deleted of the *slt70* gene	This study
17-2Δ*2762*	17-2 deleted of the *EC042_2762* gene	This study
17-2Δ*etgA*	17-2 deleted of the *etgA* gene	This study
17-2 sfGFP-TssM	sfGFP inserted after the start codon of the *tssM* gene in 17-2	Durand *et al.*, 2015
17-2Δ*mltE* sfGFP-TssM	17-2 sfGFP-TssM deleted of the *mltE* gene	This study

Plasmids

Vectors	Description	Source
Vectors for chromosomal insertions		
pKD4	One-step gene inactivation vector, Kan^R	Datsenko & Wanner, 2000
pKOBEG	Recombination vector, phage *λ recγβα* operon under the control of the pBAD promoter, Cm^R	Chaveroche *et al.*, 2000
Expression vectors		
pUA66-*rrnb*	P_{rrnB} *::gfpmut2* transcriptional fusion in pUA66, Kan^R	Zaslaver *et al.*, 2006
pASK-IBA37(+)	cloning vector, P*tet*, f1 origin, Amp^R	IBA Technology
pASK-IBA37-$_{FLAG}$TssM	*sci-1 tssM* carrying N-terminal FLAG tag cloned into pASK-IBA37(+)	Aschtgen *et al.*, 2010
pASK-IBA4	cloning vector, P*tet*, OmpA signal sequence, f1 origin, Amp^R	IBA Technology
pASK-IBA4-TssMp	*sci-1 tssM* periplasmic domain (aa 386-1129), cloned into pASK-IBA4, N-terminal FLAG epitope	Felisberto-Rodrigues *et al.*, 2011
pASK-IBA4-TssM$_{386-973}$	*sci-1 tssM* periplasmic fragment (aa 386-973), cloned into pASK-IBA4, N-terminal FLAG epitope	Felisberto-Rodrigues *et al.*, 2011
pASK-IBA4-TssM$_{972-1129}$	*sci-1 tssM* periplasmic fragment (aa 972-1129), cloned into pASK-IBA4, N-terminal FLAG epitope	Felisberto-Rodrigues *et al.*, 2011
pMS600	cloning vector, pOK12 derivative, P*lac*, P15A origin, Kan^R	Aschtgen *et al.*, 2008
pMS-Hcp$_{HA}$	*sci-1 hcp* gene cloned into pMS600, C-terminal HA epitope	Aschtgen *et al.*, 2010
pMS-TssJ$_{HA}$	*sci-1 tssJ* gene cloned into pMS600, C-terminal HA epitope	Aschtgen *et al.*, 2008
pMS-TssL$_{HA}$	*sci-1 tssL* gene cloned into pMS600, C-terminal HA epitope	Aschtgen *et al.*, 2012
pUC12	cloning vector, P*lac*, ColE1 origin, Amp^R	Norrander *et al.*, 1983
pUC-Hcp$_{FLAG}$	*sci-1 hcp* gene cloned into pUC12, C-terminal FLAG epitope	Aschtgen *et al.*, 2008
pBAD33	cloning vector, *Para*, *araC,* p15A origin, Cm^R	Guzman *et al.*, 1995
pBAD33-MltE$_{VSV-G}$	*mltE* gene cloned into pBAD33, C-terminal VSV-G epitope	This study
pBAD33-MltE^{E64Q}	*mltE* Glu64-to-Gln mutation introduced in pBAD33-MltE$_{VSV-G}$, C-terminal VSV-G epitope	This study
pETG20A	Gateway® destination cloning vector, *PT7*, N-terminal 6×His tag, TEV clivage sequence, ColE1 origin, Amp^R	Arie Gerlof
pETG20A-TssMp	*sci-1 tssM* periplasmic domain (aa 386-1129), cloned into pETG20A	Felisberto-Rodrigues *et al.*, 2011
pBADnLIC	cloning vector, *Para*, *araC*, N-terminal 10×His tag, TEV clivage sequence, P15A origin, Amp^R	Geertsma & Poolman, 2007
pBADnLIC-sMltE	*mltE* gene lacking its signal sequence cloned into pBADnLIC	Fibriansah *et al.*, 2012
pBADnLIC-MltE^{E64Q}	*mltE* Glu64-to-Gln mutation introduced in pBADnLIC-MltE	Fibriansah *et al.*, 2012
Bacterial two-hybrid vectors		
pT18-FLAG	bacterial two hybrid vector, ColE1 origin, P*lac*, T18 fragment of *Bordetella pertussis* CyaA, Amp^R	Battesti & Bouveret, 2008

pT18-MltA	*mltA* gene lacking its signal sequence cloned downstream T18 in pT18-FLAG	This study
pT18-MltB	*mltB* gene lacking its signal sequence cloned downstream T18 in pT18-FLAG	This study
pT18-MltC	*mltC* gene lacking its signal sequence cloned downstream T18 in pT18-FLAG	This study
pT18-MltD	*mltD* gene lacking its signal sequence cloned downstream T18 in pT18-FLAG	This study
pT18-MltE	*mltE* gene lacking its signal sequence cloned downstream T18 in pT18-FLAG	This study
pT18-MltE^{E64Q}	*mltE* Glu64-to-Gln mutation introduced in pT18-MltE	This study
pT18-Slt70	*slt70* gene lacking its signal sequence cloned downstream T18 in pT18-FLAG	This study
pT18-2762	*EC042_2762* gene lacking its signal sequence cloned downstream T18 in pT18-FLAG	This study
pT18-EtgA	*etgA* gene lacking its signal sequence cloned downstream T18 in pT18-FLAG	This study
pT18-Pal	*pal* gene lacking its signal sequence cloned downstream T18 in pT18-FLAG	Battesti & Bouveret, 2008
pT25-FLAG	bacterial two hybrid vector, P15A origin, P*lac*, T25 fragment of *Bordetella pertussis* CyaA, Kan^R	Battesti & Bouveret, 2008
pT25-VgrG	*sci-1 vgrG* gene cloned downstream T25 in pT25-FLAG	Zoued *et al.*, 2013
pT25-TssJ$_{sol}$	*sci-1 tssJ* gene lacking its signal sequence cloned downstream T25 in pT25-FLAG	Zoued *et al.*, 2013
pT25-TssMp	*sci-1 tssM* periplasmic domain (amino-acids 386-1129) cloned downstream T25 in pT25-FLAG	Zoued *et al.*, 2013
pT25-TagLp	*sci-1 tagL* periplasmic domain (amino-acids 352-576) cloned downstream T25 in pT25-FLAG	This study
pTolB-T25	*tolB* gene cloned upstream T25 in pT25-FLAG	Battesti & Bouveret, 2008

Oligonucleotides

Name	Destination	Sequence (5' to 3')
For chromosomal mutant strain construction [a]		
5-Del-mltA-DW	*mltA* gene deletion	CGGTTTGTTATCTTCGTTGCGCCTTATTTTTTAACCTGAAGAAGAGAACATGTGTAGGCTGGAGCTGCTTCG
3-Del-mltA-DW	*mltA* gene deletion	TTACCCCTCACCCTGTCATATCCGTAAAAACGGCATACAGAATATCACACATATGAATATCCTCCTTAGTTC
5-Del-mltB-DW	*mltB* gene deletion	TGATGCTTTACCATACTTGCCCCTGGTTGAATCTGTTAAATGGACCCCTCTGTGTAGGCTGGAGCTGCTTCG
3-Del-mltB-DW	*mltB* gene deletion	AAAAGCTGATTAGCCAGAGGGAAGCTCACGCTCCCCTCTTGCAAATAGCATATGAATATCCTCCTTAGTTC
5-Del-mltC-DW	*mltC* gene deletion	GCACGCCTCCGGCAACTTGCATAAAAACAAACACAACACGCACCCGGATGTGTAGGCTGGAGCTGCTTCG
3-Del-mltC-DW	*mltC* gene deletion	TGTGGATAACATTTTTGCCCCTGAGCATCGTCAGGGGCGGTTAATGGAACATATGAATATCCTCCTTAGTTC
5-Del-mltD-DW	*mltD* gene deletion	TCCGTTCGCCGTTATGATCGGTCGTCTTTTAAGCAACTATTGACACACACTGTGTAGGCTGGAGCTGCTTCG
3-Del-mltD-DW	*mltD* gene deletion	AAATAAAAAAGGCACCGGGGGAATCGGTGCCTTTTTATTATCTGGTTTGCATATGAATATCCTCCTTAGTTC
5-Del-mltE-DW	*mltE* gene deletion	TGTGCCGTTGTCACCTCAACGGCGATTCCAGGCTATAAGGATAGAAGAATGTGTAGGCTGGAGCTGCTTCG
3-Del-mltE-DW	*mltE* gene deletion	CTCTCGAGCGGGAAGCCCGGGAGAAAGCGGACAAAGTGCGCGACTGATCATATGAATATCCTCCTTAGTTC
5-Del-slt70-DW	*slt70* gene deletion	TTACGCGGCATGACGCTGCATTGATGTATTTACACTTAGAGGATGCGCTTTGTGTAGGCTGGAGCTGCTTCG

3-Del-slt70-DW	*slt70* gene deletion	CCGGTTGTACTCGCTAAAGAGTACGATAGCATATCATAAACGTGCGGACATATGAATATCCTCCTTAGTTC
5-Del-2762-DW	*EC042_2762* gene deletion	TTATTACGTTTTTTCAAGCTGGGACGCGCACGACACAGAGAATTAACTAATGTGTAGGCTGGAGCT GCTTCG
3-Del-2762-DW	*EC042_2762* gene deletion	ATGCGCCGCCAGGAAATTAAAGCGCAGAAAAAAGCGCGATCCTCGACGGACATATGAATATCCTC CTTAGTTC
5-Del-etgA-DW	*etgA* gene deletion	GATTATATTAGTATCTCGTTCCTTTCCTTCAATCCTACACATAAAAATATTGTGTAGGCTGGAGCTGCTTCG
3-Del-etgA-DW	*etgA* gene deletion	AGCTTTACGTATGGGTGTTTGCACTATATAAAAAAAAGAGGCTTTAGGCCATATGAATATCCTCCTTAGTTC

For plasmid construction [b,c]

5-pBAD-MltE$_{VSV-G}$	insertion of *mltE* into pBAD33	CTCTCTACTGTTTCTCCATACCCGTTTTTTTGGGCTAGCAGGAGGTATTACACCATGAAATT AAGATGGTTTGCCTTTTTGATTGTG
3- pBAD-MltE$_{VSV-G}$	insertion of *mltE* into pBAD33	GGTCGACTCTAGAGGATCCCCGGGTACCTTA*TTTTCCTAATCTATTCATTTCAATATCTGTATA*C ATCGCGTCCAGTGCCTGC
T18N-5-MltA	insertion of signal sequence-less *mltA* into pT18-FLAG	CGCCACTGCAGGGATTATAAAGATGACGATGACAAGTCTTCCAAACCAAC CGATCGCG
T25T18N-3-MltA	insertion of signal sequence-less *mltA* into pT18-FLAG	CGAGGTCGACGGTATCGATAAGCTTGATATCGAATTCTAGTTAGCCGCTA AAGACGTTACCTGCG
T18N-5-MltB	insertion of signal sequence-less *mltB* into pT18-FLAG	CGCCACTGCAGGGATTATAAAGATGACGATGACAAGAGCAGCAAGCCAA AACCTACTGAG
T25T18N-3-MltB	insertion of signal sequence-less *mltB* into pT18-FLAG	CGAGGTCGACGGTATCGATAAGCTTGATATCGAATTCTAGTTACTGCACG CGCGCCAG
T18N-5-MltC	insertion of signal sequence-less *mltC* into pT18-FLAG	CGCCACTGCAGGGATTATAAAGATGACGATGACAAGTCGACGACCAAAA AAGGCGATACC
T25T18N-3-MltC	insertion of signal sequence-less *mltC* into pT18-FLAG	CGAGGTCGACGGTATCGATAAGCTTGATATCGAATTCTAGTTATCGGCGG CGGTAGGATTTTTG
T18N-5-MltD	insertion of signal sequence-less *mltD* into pT18-FLAG	CGCCACTGCAGGGATTATAAAGATGACGATGACAAGCAGAGTACCGGCA ACGTTCAAC
T25T18N-3-MltD	insertion of signal sequence-less *mltD* into pT18-FLAG	CGAGGTCGACGGTATCGATAAGCTTGATATCGAATTCTAGTTAGGAATCT GGCATGTTGTTGTTTTTCACAAAC
T18N-5-MltE	insertion of signal sequence-less *mltE* into pT18-FLAG	CGCCACTGCAGGGATTATAAAGATGACGATGACAAGTCATCAAAGCATGA CTACACGAACCC
T25T18N-3-MltE	insertion of signal sequence-less *mltE* into pT18-FLAG	CGAGGTCGACGGTATCGATAAGCTTGATATCGAATTCTAGTTACATCGCGT CCAGTGCCTG
T18N-5-Slt70	insertion of signal sequence-less *slt70* into pT18-FLAG	CGCCACTGCAGGGATTATAAAGATGACGATGACAAGGCGCGAGCCGACT CACTG
T25T18N-3-Slt70	insertion of signal sequence-less *slt70* into pT18-FLAG	CGAGGTCGACGGTATCGATAAGCTTGATATCGAATTCTAGTTAGTAACGA CGTCCCCATTCCGTG

T18N-5-2762	insertion of signal sequence-less *EC042_2762* into pT18-FLAG	CGCCACTGCAGGGATTATAAAGATGACGATGACAAGGCTCTCTGG CCATCCATTCC
T25T18N-3-2762	insertion of signal sequence-less *EC042_2762* into pT18-FLAG	CGAGGTCGACGGTATCGATAAGCTTGATATCGAATTCTAGTTAAT TTTGTTTCTCTTCACTCCCTTTCCTGG
T18N-5-EtgA	insertion of signal sequence-less *etgA* into pT18-FLAG	CGCCACTGCAGGGATTATAAAGATGACGATGACAAGGCCAGTAGCGCTTG CTTTAATGAAGC
T25T18N-3-EtgA	insertion of signal sequence-less *etgA* into pT18-FLAG	CGAGGTCGACGGTATCGATAAGCTTGATATCGAATTCTAGTTATTTTGCTA AAGCCTTACGCTTGTCTATTTC
T25N-5-TagLp	insertion of $tagL_{352\text{-}576}$ fragment into pT25-FLAG	GGCGGGCTGCAGATTATAAAGATGACGATGACAAGCGGCTGGTTCGCAGC GTG
T25T18N-3-TagLp	insertion of $tagL_{352\text{-}576}$ fragment into pT25-FLAG	CGAGGTCGACGGTATCGATAAGCTTGATATCGAATTCTAGTTACTCCGTT ATGTTTTCTGATGCGCC
For site-directed mutagenesis [d]		
A-MltE-E64Q	Glu64-to-Gln mutation in *mltE*	GGCGATTATCGCTATC**CAA**TCGGGTGGTAATCC
B-MltE-E64Q	Glu64-to-Gln mutation in *mltE*	GGATTACCACCCGA**TTG**GATAGCGATAATCGCC

[a] Sequences corresponding to the downstream and upstream regions of the gene to be deleted underlined
[b] Sequence annealing on the target plasmid underlined.
[c] FLAG or VSV-G epitope coding sequence *italicized*.
[d] Mutagenesized codon in **Bold.**